Carbohydrate Polymers 89 (2012) 640–647

Contents lists available at SciVerse ScienceDirect

Carbohydrate Polymers

journal homepage: www.elsevier.com/locate/carbpol

Hydration properties of regioselectively etherified celluloses monitored by ^{2}H and ^{13}C solid-state MAS NMR spectroscopy

Flemming H. Larsen[a,*], Michael Schöbitz[b,c], Jens Schaller[b]

[a] Department of Food Science, University of Copenhagen, Rolighedsvej 30, DK-1958 Frederiksberg C, Denmark
[b] Thüringisches Institut für Textil- und Kunststoff-Forschung e. V., Eingetragener Verein, Breitscheidstraße 97, 07407 Rudolstadt, Germany
[c] Institute of Organic Chemistry and Macromolecular Chemistry, Center of Excellence for Polysaccharide Research, Humboldtstraße 10, D-07743 Jena, Germany

ARTICLE INFO

Article history:
Received 5 January 2012
Received in revised form 19 March 2012
Accepted 20 March 2012
Available online 29 March 2012

Keywords:
2,3-O-hydroxypropylcellulose
2,3-O-hydroxyethylcellulose
Solid-state
NMR
Hydration
Regioselective

ABSTRACT

The hydration properties of 2,3-O-hydroxypropylcellulose (HPC) and 2,3-O-hydroxyethylcellulose (HEC) were analyzed by multi-nuclear solid-state MAS NMR spectroscopy. By ^{13}C single-pulse (SP) MAS and cross-polarization (CP) MAS NMR, differences between the immobile regions and all parts of the polysaccharides were detected as a function of hydration. Complementary information about the water environments was observed by ^{2}H MAS NMR. By this approach it was demonstrated that side chains in 2,3-O-HPC and 2,3-O-HEC were easier to hydrate than the cellulose backbone. Furthermore the motion of water was more restricted (slower) in 2,3-O-HPC than in 2,3-O-HEC. For both polysaccharides the hydration could be explained by a two-step process: in step one increased ordering of the immobile regions occurs after which the entire polymer is hydrated in step two.

1. Introduction

As the most abundant biopolymer in nature increasing attention is paid to cellulose and its derivatives. Cellulose itself is used as a source of fibres and paper, as well as a packaging material in polymer blends (Klemm, Philipp, Heinze, Heinze & Wagenknecht, 1998). An even broader range of applications exists for cellulose derivatives. Cellulose esters like cellulose acetates or butyrates are used as thermoplastic polymer for fibres, LC-displays and filter tows (Edgar et al., 2001). Another important reaction used for cellulose derivatization is etherification. Cellulose ethers like carboxymethyl-, ethyl-, methyl-, hydroxyethyl-, hydroxypropyl-cellulose and mixtures thereof are commonly used as thickeners in the construction and food industry (Chang & Zhang, 2011; Knaus & Bauer-Heim, 2003). The physicochemical properties of cellulose ethers like viscosity, solubility or flocculation behavior depend strongly on the distribution of the substituents along the cellulose chain and the substitution pattern of the three hydroxyl groups in the repeating anhydroglucose unit (AGU) (Kondo, 1997). The reactivity of the hydroxyl groups for heterogeneous etherification reactions depends on the reagents used. For etherification with short alkyl chains and carboxymethylation the reactivity is C-2 > C-6 > C-3 (Baar, Kulicke, Szablikowski & Kieswetter, 1994; Dönges, 1990). In the case of hydroxyethylethers the preference for the C-2 position diminishes. By using a high alkali content C-6 substitution is preferred, applying low alkali content the C-2 position is preferred. In the case of hydroxypropylation the reactivity is C-6 > C-2 > >C-3 (Dönges, 1990; Wirick, 1968). Our aim was to investigate hydration properties of 2,3-O-hydroxethyl cellulose (HEC) and 2,3-O-hydroxypropyl cellulose (HPC) prepared by the well known protecting group technique (Schaller & Heinze, 2005).

The investigation of the hydration properties of 2,3-O-HEC and 2,3-O-HPC was performed by solid state NMR. Previously this analytical technique was used to analyze cellulose in various forms (Earl & VanderHart, 1981; VanderHart & Atalla, 1984; Witter et al., 2006), cellulose derivatives (Hoshino, Takai, Fukuda, Imura & Hayashi, 1989), assess hydration properties in intact plant cell walls (Ha, Viëtor, Jardine, Apperley & Jarvis, 2005; Hediger, Emsley & Fischer, 1999) and also native and modified rhamnogalacturonan-I (RG-I) from potato cell walls (Larsen et al., 2011). The latter study employed ^{13}C single-pulse (SP) magic angle spinning (MAS), ^{13}C cross polarization (CP) MAS as well as ^{2}H SP/MAS NMR experiment to assess hydration properties in RG-I using D_2O as a source of hydration. This approach provided information about hydration effects of the polysaccharide as well as the mobility of water. In the present study an identical experimental approach will be employed. During the hydration process the polysaccharides are neither in the solid or in the liquid state but in an intermediate state

* Corresponding author. Tel.: +45 3533 3501; fax: +45 3533 3245.
E-mail address: fhl@life.ku.dk (F.H. Larsen).

0144-8617/$ – see front matter © 2012 Elsevier Ltd. All rights reserved.
http://dx.doi.org/10.1016/j.carbpol.2012.03.067

often referred to as suspension. For this reason both ^{13}C CP/MAS and ^{13}C SP/MAS experiments will be used as the resonances of the carbons in the immobile (rigid) regions of the polymer will be enhanced by CP, whereas all carbons will be observed quantitatively correct by the SP/MAS experiments.

2. Materials and methods

The microcrystalline cellulose powder (20 μm) was purchased from Sigma–Aldrich (Sigma 310697) and used without further purification.

The cellulose material used for synthesis of cellulose ethers was spruce sulfite pulp with a degree of polymerization (DP) of 650. It was dried in vacuum for 2 h at 100 °C before use. 2-Propanol, sodium dodecyl sulfate (SDS) and IMBENTIN AGS-35 (25% solution of poly(ethylene glycol) C11–C15 ether in water) were obtained from Fluka. Ethylene oxide (EO) and propylene oxide (PO) were purchased from Gerling, Holz &Co, Hanau, Germany. All reactions were carried out into a 2 l stainless steel reactor (Karl Kurt, Juchheim, Germany). The 6-O-(4-monomethoxytrityl) cellulose (MMTC) was prepared by reacting cellulose dissolved in N,N-dimethylacetamide (DMAc)/LiCl with 4-monomethoxytrityl chloride/triethylamine at 70 °C for 24 h according to reference (Gomez, Erler, & Klemm, 1996).

2.1. Synthesis of 2,3-O-HPC and 2,3-O-HEC

2.1.1. Heterogeneous hydroxyethylation of MMTC

A mixture of 5 g of MMTC was suspended in 100 ml of 2-propanol/water mixture (75/25). The suspension was stirred and treated with 4 ml 50% NaOH (resulting in a 10% NaOH concentration) and 0.5 g of a detergent mixture, consisting of 1 part SDS and 2 parts IMBENTIN-AGS-35. The reaction mixture was stirred for 30 min at 40 °C. 20 g EO were added and the temperature was increased to 70 °C. The reaction mixture was stirred for 3 h at 70 °C before it was cooled down to room temperature and the reactor was flushed with argon four times. The raw material was dissolved in 75 ml tetrahydrofuran (THF) and re-precipitated in 750 ml water. To remove the detergent, the precipitate was washed additionally with 3 l distilled water. After washing with 75 ml ethanol the product was dried in vacuum at 50 °C. Yield: 5.8 g.

The *hydroxypropylation* of 5 g MMTC was carried out in a similar manner applying 27 g PO. Yield: 5.5 g.

2.1.2. Detritylation of 2,3-O-hydroxyalkyl-6-O-(4-monomethoxytrityl) celluloses

The 2,3-O-hydroxyalkyl-6-O-(4-monomethoxytrityl) celluloses were detritylated by stirring 5 g of the sample in a mixture of 200 ml ethanol and 10 ml concentrated aqueous HCl for 16 h at room temperature. The products were filtrated off and washed with 80% aqueous ethanol (until neutral reaction) and with pure ethanol. The samples were dried in vacuum at 50 °C.

2,3-O-Hydroxyethyl cellulose (2,3-O-HEC): yield: 2.0 g, $MS_{HE} = 0.39$ (calculated from ^1H NMR spectrum of the peracetylated product). ^{13}C NMR (DMSO-d_6): $\delta = 101.6$ (C-1), 101.0 (C-1), 81.7 (C-2s, C-3s), 79.8 (C-4), 75.2–74.0 (C-2, C-3, C-5), 74.1 (C-8), 72.2 (C-7), 69.7 (C-7), 60.2 (C-9), 60.1 (C-6).

2,3-O-Hydroxypropyl cellulose (2,3-O-HPC): yield: 4.9 g, $MS_{HP} = 0.61$ (calculated from ^1H NMR spectrum of the peracetylated product). ^{13}C NMR (DMSO-d_6): $\delta = 18.8$ and 19.2 ppm (C-9), 19.7 (C-12), 16.8 (C-9), 64.4–65.3 (C-8 and C-11), 74.5 (C-8) and carbons of the sugar unit).

2.1.3. Peracetylation of 2,3-O-HEC and 2,3-O-HPC

0.5 g of 2,3-O-HEC (or HPC) were suspended in 15 ml pyridine and treated with 15 ml acetic anhydride and 0.02 g 4-(N,N-dimethylamino) pyridine. After stirring overnight the mixture was heated to 60 °C for 4 h and poured into 200 ml water containing about 10% $NaHCO_3$. The precipitated polymer was collected, washed with water and dried in vacuum at 50 °C. Yield: 0.5 g.

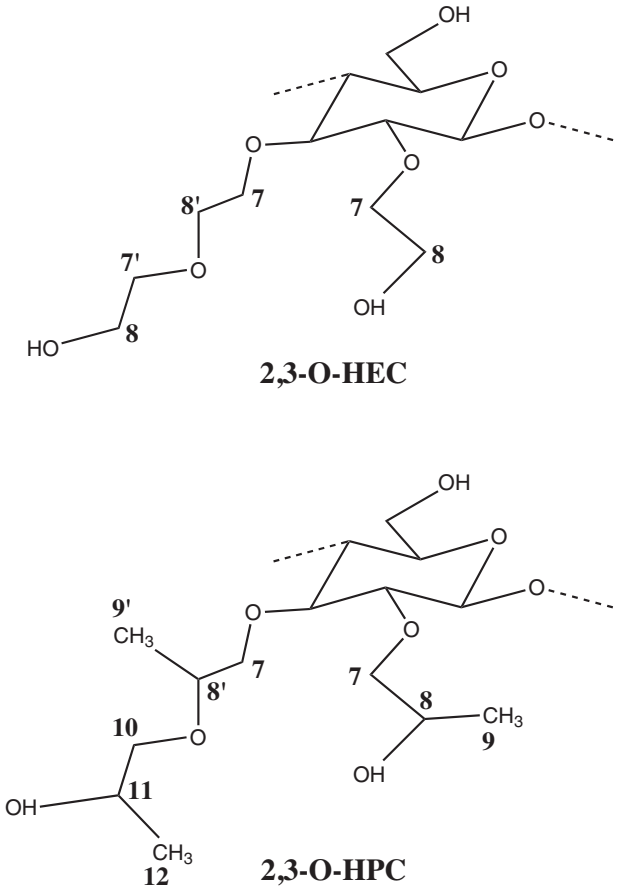

Fig. 1. Structures of 2,3-O-HPC and 2,3-O-HEC.

The polymer is soluble in chloroform and dimethylsulfoxide (DMSO). FT-IR (KBr): no ν_{OH}, 1754 cm^{-1} ($\nu_{C=O}$). ^1H NMR ($CDCl_3$): $\delta = 5.1–2.9$ [anhydroglucose unit (AGU)-protons, CH_2- and CH-protons of hydroxyalkyl substituents], 2.1–1.9 ppm (CH_3-protons of acetyl groups), 1.0–1.2 (CH_3-protons of hydroxypropyl substituents).

Schematic structures of these are shown in Fig. 1.

2.1.4. Measurements

The determination of the degree of substitution (DS) of MMT groups was carried out by elemental analysis. The molar degree of substitution (MS) of hydroxyethyl and hydroxypropyl substituents was determined by ^1H NMR spectroscopy of the peracetylated products. The NMR spectra were recorded on a Bruker DRX 400 spectrometer. ^{13}C NMR spectra were measured in $CDCl_3$ or DMSO-d_6. 4700–18,000 scans were accumulated. For the ^1H NMR spectra 16 scans were accumulated. FTIR spectra were recorded on a BioRad FTS 25 spectrometer (KBr-technique).

2.2. Solid-state and two-dimensional NMR spectroscopy

The solid-state NMR experiments were performed using a Bruker Avance 400 spectrometer (9.4 T) operating at 400.13, 100.62 and 61.42 MHz for ^1H, ^{13}C and ^2H respectively, employing a double tuned solid-state probe equipped with 4 mm (o.d.) spinners. The ^{13}C single-pulse (SP) MAS and cross-polarization (CP) MAS

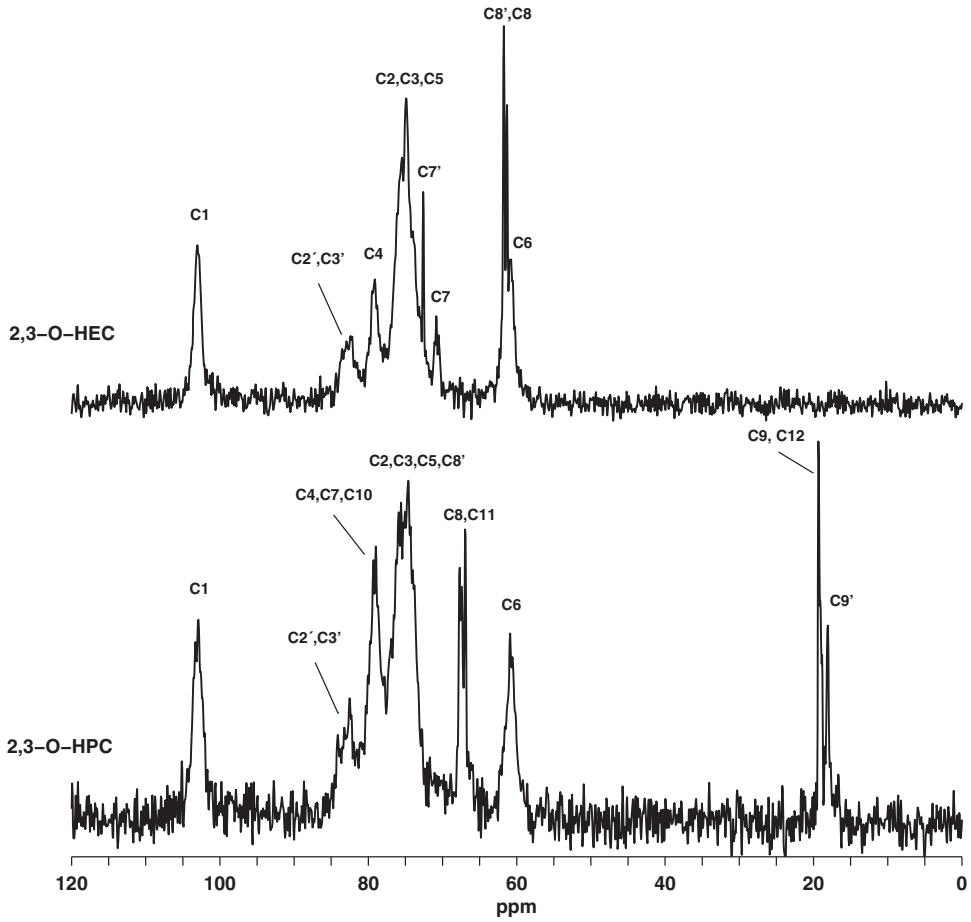

Fig. 2. Assignment of resonances in ^{13}C SP/MAS spectra of HPC and HEC, hydration level = 70%.

spectra were recorded using ^{1}H and ^{13}C rf-field strengths of 80 kHz and a spin-rate of 8 kHz (11 kHz for cellulose). Acquisition times of 40.9 ms were employed and during (ramped) cross-polarization (Metz, Wu & Smith, 1994) a contact time of 1 ms was used. High power ^{1}H decoupling was obtained via the TPPM decoupling scheme (Bennett, Rienstra, Auger, Lakshmi, Griffin, 1995). Recycle delays of 16 and 256 s were employed for the CP/MAS and SP/MAS experiments, respectively. These recycle delays were optimized on the dry samples and used for the hydrated samples. Typical number of scans was 1024 (4000 for most dilute samples) for the CP/MAS spectra and 920 for the SP/MAS spectra. All spectra were referenced (externally) to the carbonyl resonance in α-glycine at 176.5 ppm. The spectra were apodized by Lorentzian linebroadenings of 1 Hz. Fitting of line widths using a Lorentzian lineshape was performed by the built-in procedure in the Topspin 2.1 software. The hydrated samples were prepared by weighing out the powder in the rotor and subsequently adding D_2O using a Hamilton Microliter® #810 syringe. In order to avoid removal of hydrated polysaccharide from the rotor, it is important to release D_2O onto the powder surface and continuously release D_2O while inserting the needle into the powder along the inner wall of the rotor to assure that the needle is surrounded by D_2O at all times. Likewise D_2O must be continuously released while the needle is removed from the rotor. Prior to acquisition the hydrated samples had been spinning at 8 kHz (11 kHz for cellulose) for at least 1 h to ensure proper mixing of powder and D_2O. Due to the delicate spinning module in the NMR probe stable spinning was only achieved when the sample was homogenously distributed within the rotor. This also ensured a proper mixture of powder and D_2O. In this study D_2O volumes of 45, 56, 65 and 75 μl, respectively, were used. The degree of hydration for each sample is supplied in weight-% ($= 100\% \times m_{D_2O}/(m_{D_2O} + m_{powder})$).

^{2}H single-pulse (45 degree flip angle) MAS experiments were recorded using a spin-rate of 2 kHz, 4096 scans, a recycle delay of 1 s and an acquisition time of 27.3 ms during which ^{1}H TPPM decoupling (80 kHz rf-field strength) was employed. All ^{2}H MAS FIDs were apodized by Lorentzian linebroadenings of 0.3 Hz prior to Fourier transformation. Fitting of the centerband using a Lorentzian lineshape was performed by the built-in procedure in the Topspin 2.1 software.

The liquid-state NMR experiments were performed using a Bruker Avance III 600 spectrometer (14.1 T) operating at 600.13 and 150.91 MHz for ^{1}H and ^{13}C, respectively. Samples (0.76 mg 2,3-O-HPC or 0.86 mg 2,3-O-HEC in 550 μl D_2O with 5.8 mM TSP-d4) were analyzed by 2D homonuclear (^{1}H–^{1}H) COSY and TOCSY (70 ms mixing time) experiments as well as heteronuclear ^{1}H–^{13}C HSQC (with or without spectral editing) experiments using a TCI cryoprobe equipped for 5 mm (o.d.) sample tubes. Assignment of the 2D NMR spectra was performed using Sparky 3.114 (Goddard & Kneller, 2007). This assignment was used to support the assignment of the solid-state NMR spectra.

All NMR experiments were conducted at room temperature.

3. Results and discussion

In Fig. 2 ^{13}C SP/MAS spectra of 2,3-O-HPC (hereafter: HPC) and 2,3-O-HEC (hereafter: HEC) samples at a hydration level of 70% are displayed. The assignments are indicated on the figure and also in Table 1. The main structural feature of these derivatives, namely the

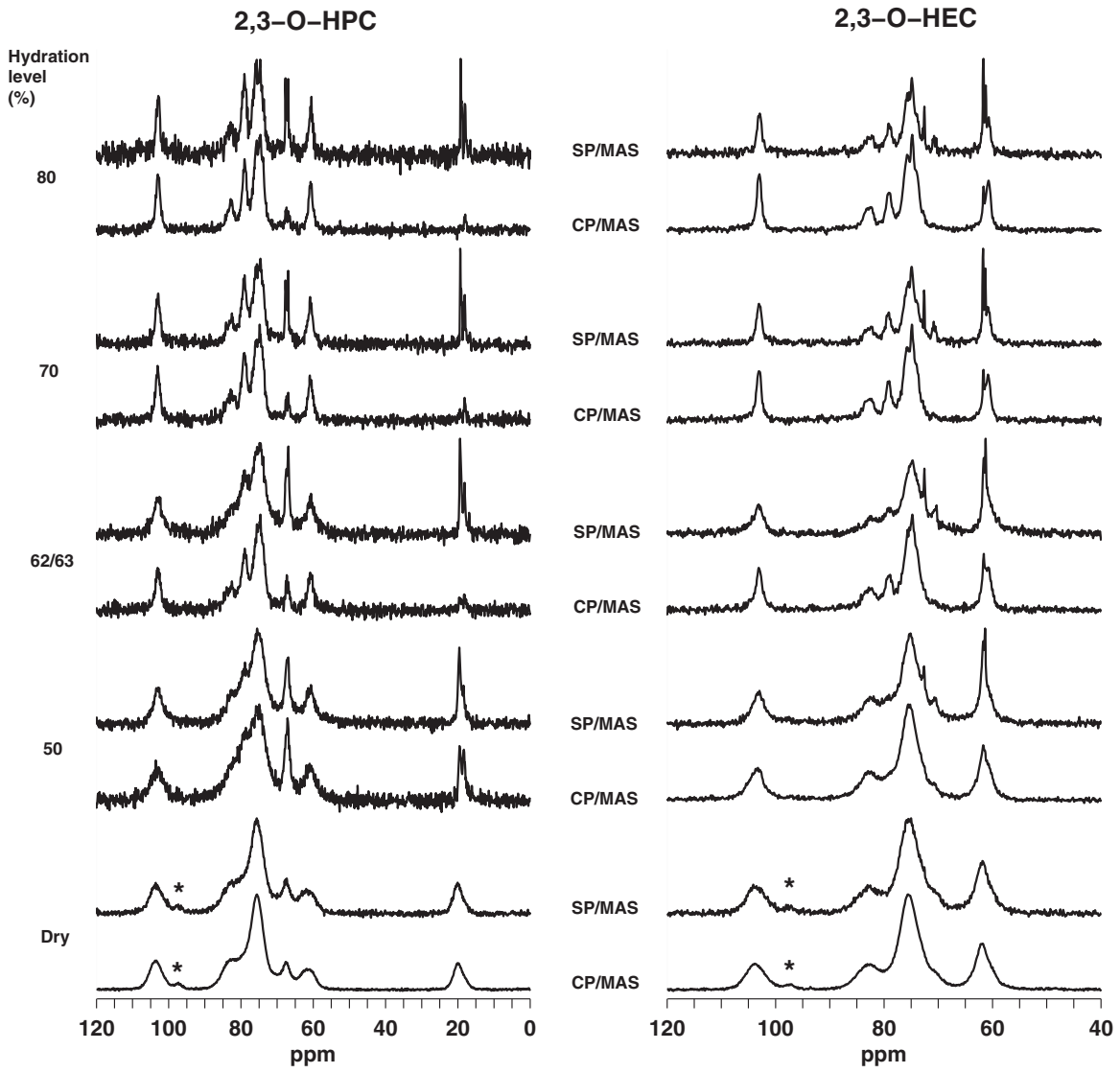

Fig. 3. ^{13}C CP/MAS (lower spectra) and SP/MAS (upper spectra) spectra of HPC (left column) and HEC (right column) at various hydration levels. In the spectra of the dry powders the resonance from C1(2*) is marked by an asterisk.

substitution only at position 2 and 3, is clearly observed in the spectra for C6 resonance. This resonance is not split or shifted, therefore indicating that position 6 is not substituted. Regarding hydration the difference in line widths when comparing resonances from the cellulose backbone (C1–C6) and resonances from the side chains (C7–C12) reflects different hydration properties. The narrower resonances from the side chains reflect that these are more mobile than the cellulose backbone. Furthermore the cellulose parts of the spectra are similar and the main differences are due to resonances from the side chains. For HEC the chemical shifts for C7 and C7′ differ significantly from C1–C6 in cellulose, whereas the C8 and C8′ resonances overlap with C6 in cellulose. In the spectrum of HPC significant spectral overlaps between C4, C7 and C10 as well as between C2, C3, C5 and C8′ were observed. On the contrary C8 and C11 as well as the resonances from the methyl groups (C9, C9′ and C12) served as clear markers for the presence of hydroxypropyl side chains.

3.1. Hydration effects

Fig. 3 displays ^{13}C CP/MAS and SP/MAS spectra of HPC and HEC at different hydration levels. Overall it is observed that the line width of the resonances is reduced upon increased level of hydration. In the dry state the SP/MAS and CP/MAS spectra are

Table 1
Tentative assignment of ^{13}C resonances in 2,3-O-HPC and 2,3-O-HEC (70% hydration level) from solid-state ^{13}C MAS NMR spectra. When both C*n* and C*n*′ exist the chemical shift for C*n* is mentioned at first. The chemical shifts for C1 (2*) in the dry samples are listed below the chemical shift for C1.

Monomer/nucleus	C1	C2	C3	C4	C5	C6	C7	C8	C9	C10	C11	C12
2,3-O-HPC (this work)	103.3/97.3	73–77/82–84	73–77	79	73–77	60.8	79	67.5/73–77	19.3/18.1	79	67.0	19.3
2,3-O-HEC (this work)	103.0/97.3	73–77/82–84	73–77	79.3	73–77	60.8	70.5–71/72.6	61.3/61.7				
Cellulose, I_α [a]	105.0	71.6, 70.1	74.7, 73.9	90.0, 89.1	72.6, 70.1	65.2						
Cellulose, I_β [a]	106.1, 104.0	71.3, 71.0	74.9, 74.2	88.9, 88.0	72.2, 70.6	65.6, 65.0						

[a] From Kono, Erata, and Takai (2003).

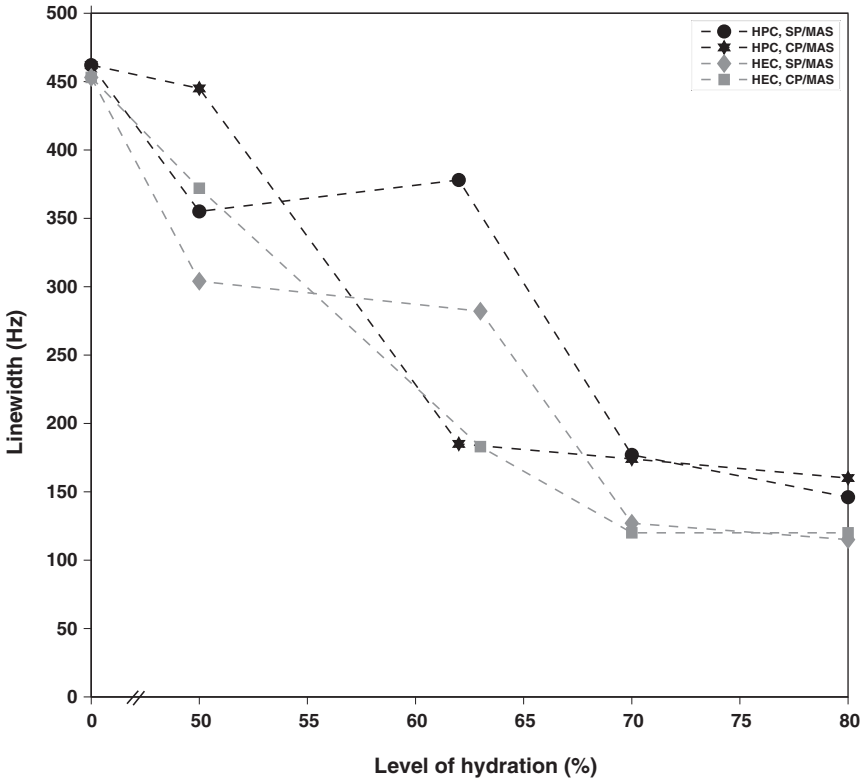

Fig. 4. Line widths for the C1 resonance in either HPC or HEC at various hydration levels by either ^{13}C CP/MAS or SP/MAS experiments. Gray symbols (diamond and square) indicate HEC and black symbols (filled circle and star) indicate HPC. Symbols are connected by dashed lines as a guide to the eye.

identical for both HPC and HEC except for a better S/N-ratio in the CP/MAS spectra. An initial effect of hydration is observed in both HPC and HEC when comparing the spectra of the dry powders with the powders having a hydration level of 50%. In the dry powder a broad resonance around 97.3 ppm is present, whereas it disappears upon hydration. Previously (Capitani, Nobile, Mensitieri, Sannino & Segre, 2000) this resonance was tentatively assigned to C1 (dubbed C1 (2*)) situated next to a C2 attached to an ether side chain. Similarly, a resonance at 95 ppm in amorphous starch has been ascribed to a high-energy, twisted conformation (Tan, Flanagan, Halley, Whittaker & Gidley, 2007). These two explanations may both apply presently since addition of an ether side chain could induce local conformational changes in the cellulose backbone. Addition of water induced a change in the chemical shift for C1(2*) such that it is similar to C1. This suggests that the geometry of the glycosidic linkages become more uniform when water is added.

Different hydration effects for HEC and HPC are observed due to the nature of their side chains. For HPC the intensity of the CH resonances (C8, C11) around 67 ppm is greatly enhanced when the hydration level is increased to 50%. Furthermore the two CH_3-resonances originating from internal (C9′) and end-groups (C9, C12) in the hydroxypropyl side chains can be distinguished. In the CP/MAS spectrum these resonances are in a 50:50 ratio whereas they are in a 34:66 (internal:end-group) ratio in the SP/MAS spectra. Assuming identical rates of cross-polarization for the two methyl groups, this reflects that – on average – only celluloses with dimeric side chains are present in the immobile regions of HPC whereas on average there are an almost equal amount of monomeric and dimeric side chains in the overall polymer. At higher levels of hydration (>60%) it is observed that the intensity of both CH- and CH_3-resonances are reduced in the CP/MAS spectra indicating a lower abundance of side chains in the immobile regions upon hydration.

Similarly for HEC it is observed that the CP/MAS spectra of the hydrated samples mainly consist of resonances from cellulose and a slight contribution from C8 resonance of the side chains characterized by chemical shift of 61.6 ppm. In the SP/MAS spectra a narrow resonance at 72.5 ppm (C7) and a broader resonance around 70.6 ppm (C7′) are present and furthermore two narrow resonances at 61.2 and 61.6 ppm – close to the C6 resonance of cellulose – are observed. All of these originate from the side chains. The C7′ and C8′ resonances are only present in the SP/MAS spectra indicating higher mobility and therefore easier hydration than for the cellulose backbone. For both HPC and HEC it is observed that a broad resonance in the range 82–84 ppm is present at hydration levels of 62% and higher except from the SP/MAS spectrum of HPC at a hydration level of 62%. This resonance originates from C2 and C3 in the etherified AGUs.

Hydration of the cellulose backbone may be estimated from the line width of the C1 resonance. In Fig. 4 the line width of this resonance as a function of hydration level is displayed for HEC and HPC from either ^{13}C CP/MAS or SP/MAS experiments. At a hydration level of 50% the line widths in the CP/MAS experiments are larger than in the SP/MAS experiments and it is furthermore noticed that the line width is larger for HPC than for HEC. At the hydration level 62/63% the line width of the C1 resonance in the CP/MAS spectra for HPC and HEC are almost identical (185 Hz) and narrower by 193 and 99 Hz, respectively, than in the corresponding SP/MAS spectra. Only low intensity resonances from ether side chains are observed in the CP/MAS spectra at this and higher levels of hydration. Therefore the broader C1 resonance in the SP/MAS spectrum indicates a broader distribution of chemical shifts – and thereby disorder – in the etherified AGUs than in the non-substituted AGUs. This result is highly surprising and is based solely on observations at the hydration level 62/63%. An explanation of this could be that a common conformation is adopted in the immobilized regions at this hydration level

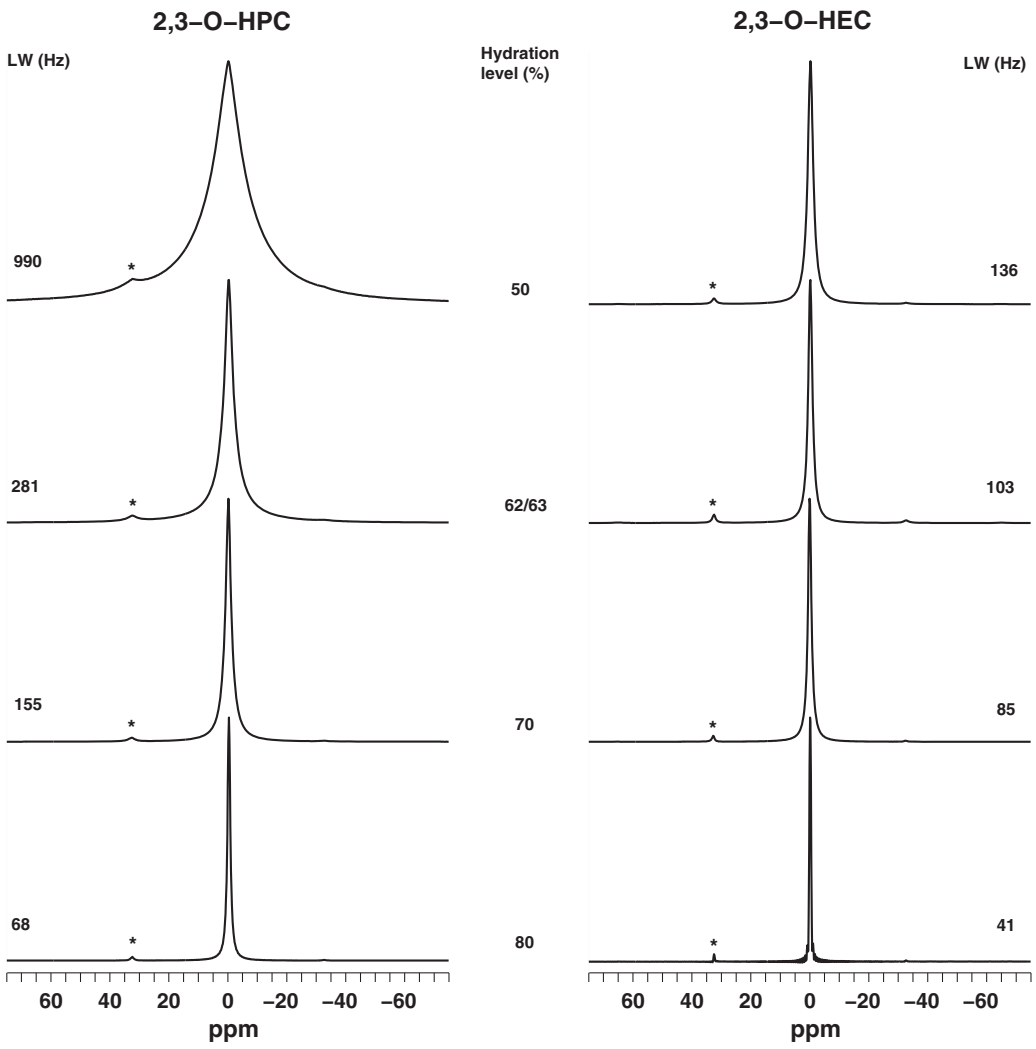

Fig. 5. ^{2}H MAS spectra of HPC (left column) and HEC (right column) at different hydration levels. Line widths (in Hz) of the center band is indicated at each spectrum. Star denotes spinning sideband.

whereas a range of evenly energetically favorable conformations may be possible in the mobile regions. The latter could be due to the higher presence of side chains in the mobile regions compared to the immobile regions. At higher levels of hydration similar line widths are observed in SP/MAS and CP/MAS experiments of the same compound, but the line width of C1 in HPC is larger than in HEC.

The hydration effects of the added D_2O were observed by ^{2}H MAS NMR spectroscopy. Some of the D_2O will exchange with OH-groups in either the cellulose backbone or the OH-groups in the ether side chains and form HDO + OD – and even H_2O. Therefore the ^{2}H MAS spectra will include observations of both D_2O, HDO and —OD groups. Since the abundance of HDO and —OD is much lower than D_2O all of the deuterium bearing compounds will subsequently be denoted D_2O. The ^{2}H MAS NMR spectra are displayed in Fig. 5 and show how the line width of the center band changes as a function of the hydration level. Going from a hydration level of 50% to 80%, the line width of the center band for HPC is reduced from 990 to 68 Hz and from 136 to 41 Hz for HEC. The difference in line widths in the ^{2}H spectra reflects differences in D_2O motion. Larger line widths at lower levels of hydration demonstrate that the motion is more restricted at lower levels of hydration. At each hydration level water motion is less restricted in HEC than in HPC. It must be noted, though, that the difference in water mobility between HEC and HPC is reduced as the hydration level is increased. This indicates that dry HPC is more tightly packed than HEC and hydrated HPC is characterized by smaller water pockets (regions) leading to more spatially restricted motion of water.

Hydration effects of C1 and the line broadening effects of D_2O suggest that the less motionally restricted D_2O environments achieved when changing the hydration level from 50 to 62/63% are due to increased ordering of the immobile regions. The presence of side chains in these regions is very low. Our results suggest that the low abundance of side chains allows for a more ordered environment at lower hydration levels whereas higher levels of hydration are required to increase the ordering in the mobile regions. In more general terms this indicates a two-step hydration process in which step one includes hydration and increased ordering of the immobile regions (low abundance of side chains) whereas the ordering of the remaining part of the system is increased in step two. Potentially the ordered immobile regions may be a necessary prerequisite to obtain the ordered structure of the entire system in step 2 of the hydration process.

3.2. Comparison of 2,3-O-HEC and 2,3-O-HPC with cellulose

In Fig. 6 it is observed that the chemical shift for C1 in cellulose is about 2.5 ppm higher than C1 in HEC and HPC. Similarly for the chemical shifts of the C4 and C6 resonances in HEC and HPC

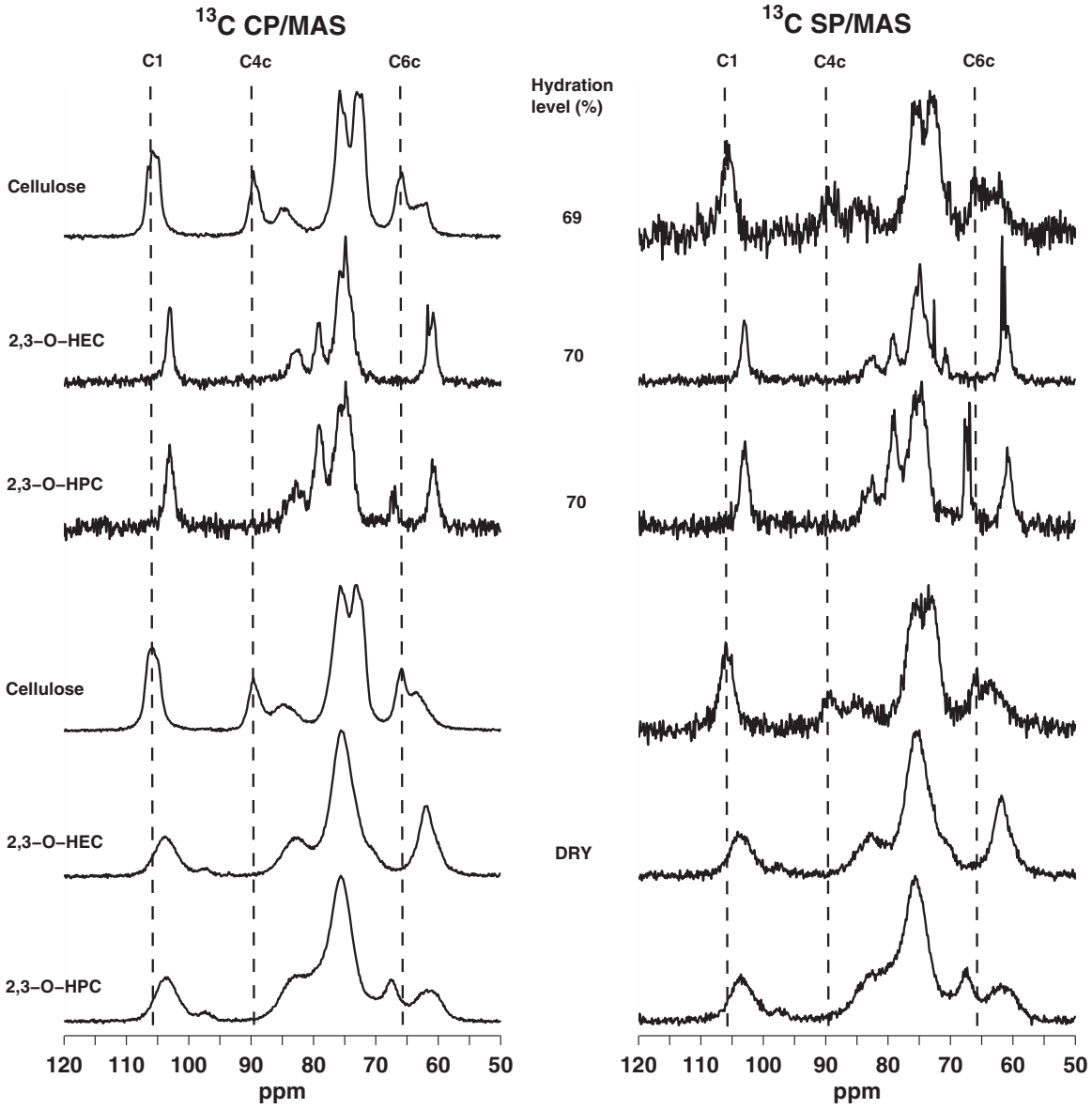

Fig. 6. ^{13}C CP/MAS (left column) and SP/MAS (right column) spectra of HPC, HEC and microcrystalline cellulose in the dry state and at a hydration level of ~70%. Resonances for C1, and C4 & C6 in crystalline cellulose are indicated by broken vertical lines.

are about 5.5 and 2.3 ppm, respectively, lower than in amorphous cellulose and ~10 ppm and 4.2 ppm lower than in crystalline cellulose. On the other hand resonances from C2 and C5 in HEC and HPC are around 2 ppm higher than in cellulose whereas the chemical shift for non-substituted C3 are similar. Furthermore the absence of distinct resonances for crystalline cellulose – particularly for C4 and C6 – in the spectra of HPC and HEC, indicates that the structure of the cellulose backbone in HPC and HEC is significantly different from crystalline cellulose.

Correlations between the torsion angles of the glycosidic linkage and the chemical shift of C1 were established for starch (Gidley & Bociek, 1988), and similar correlations may apply for cellulose. In cellulose the chemical shift for C4 seems to be an obvious marker for solubility since a change of around 10 ppm is observed when comparing crystalline cellulose to the regio-selective etherified celluloses. The C4 chemical shifts for HEC and HPC are very close to the ones reported for tri- to hexamers of β-1,4-linked glucose units (Flugge, Blank, & Petillo, 1999) which again is close to the chemical shift for C4 in the glycosidic linkage in methyl-O-cellobioside (Christensen et al., 2010). (Φ,Ψ)-Torsion angles reported from the latter study and from analysis of various crystalline forms of cellulose (Wada, Heux, Nishiyama, & Langan 2009) are displayed in Table 2. From this table it is seen that the C1-O-C4 angles in crystalline celluloses are similar to the one reported for cellotriose and only 10–13 degrees higher than in A- and B-type starch. Differences in torsion angles between crystalline cellulose and methyl-O-cellobioside are more pronounced and whereas differences in Φ-angles are around 7–19 degrees, the differences in the Ψ-angles are 111–125 degrees. This suggests that the hydration properties are highly correlated with this angle. The ^{13}C chemical shift for C4 is very sensitive to the Ψ-angle and a chemical shift around 90 ppm indicates a Ψ-angle around 90 degrees whereas a C4 chemical shift around 80 ppm indicates a Ψ-angle around 236 degrees. The general trend is: the lower the C4 chemical shift, the larger the Ψ-angle. Based on this we suggest that the cellulose backbone in 2,3-O-HEC and 2,3-O-HPC are characterized by a τ-angle of 115–118 degrees, a Φ-angle of 260–280 degrees, whereas the Ψ-angle is supposedly close to 236 degrees. In general terms,

Table 2
Chemicals shifts (C1 and C4), torsion and bond angles in starch, crystalline celluloses, methyl-O-cellobioside, and chemical shifts (C1 and C4) for 2,3-O-HPC and 2,3-O-HEC.

Compound	C1 (ppm)	C4 (ppm)	τ (degrees)	Φ (degrees)	Ψ (degrees)	Refs.
Starch (A & B)	99.3–101.5	76.0–76.2	105	335 ± 5	328 ± 5	Gidley and Bociek (1988)
Celluloses	104.7–107.0	87.3–88.6	115–118	261–273	85–99	Wada et al. (2009)
Methyl-O-cellobioside[b]	102.6	78.7	117 (cellotriose)[a]	281	236	Christensen et al. (2010)
2,3-O-HPC	103.3	79.0				This work
2,3-O-HEC	103.0	79.3				This work

τ is the C1-O4-C4 angle, Φ is the O5-C1-O1-C4 torsion angle, and Ψ is the C1-O1-C4-C3 torsion angle.
[a] Raymond, Henrissat, Qui, Kvick, and Chanzy (1995).
[b] Chemical shifts for carbons in the glycosidic bond.

"hydrophobic" environments are obtained when the Ψ-angle is around 90 degrees whereas "hydrophilic" environments require a Ψ-angle around 240 degrees.

4. Conclusions

In this work it was demonstrated that side chains in 2,3-O-HPC and 2,3-O-HEC were easier to hydrate than the cellulose backbone. Furthermore the hydration process was elucidated revealing that dimeric side chains in 2,3-O-HPC were more difficult to hydrate than monomeric side chains.

Comparison of the water association in HPC and HEC using ^{2}H NMR showed that the water motion was more restricted in HPC than in HEC due to higher viscosity. In both systems a two-step hydration process is suggested in which the first step includes increased ordering of the immobile regions which is a necessary prerequisite for hydration of the entire polymer.

From a structural point of view, comparison of torsion angles and C4 chemical shifts of crystalline cellulose and methyl-O-cellobioside suggested that the angles describing the glycosidic bonds of the cellulose backbone in 2,3-O-HEC and 2,3-O-HPC are close to (τ,Φ,Ψ) = (115–118, 260–280, ~236).

Acknowledgment

FHL gratefully acknowledges funding from the Danish Council for Strategic Research (BioFunCarb project, project no. 2108-08-0068).

References

Baar, A., Kulicke, W.-M., Szablikowski, K., & Kieswetter, R. (1994). Nuclear magnetic resonance spectroscopic characterization of carboxymethylcellulose. *Macromolecular Chemistry and Physics*, *195*, 1483–1492.
Bennett, A. E., Rienstra, C. M., Auger, M., Lakshmi, K. V., & Griffin, R. G. (1995). Heteronuclear decoupling in rotating solids. *Journal of Chemical Physics*, *103*, 6951–6958.
Capitani, D., Nobile, M. A. D., Mensitieri, G., Sannino, A., & Segre, A. L. (2000). ^{13}C solid-state NMR determination of cross-linking degree in superabsorbing cellulose-based networks. *Macromolecules*, *33*, 430–437.
Chang, C., & Zhang, L. (2011). Cellulose-based hydrogels: Present status and application prospects. *Carbohydrate Polymers*, *84*, 40–53.
Christensen, N. J., Hansen, P. I., Larsen, F. H., Folkerman, T., Motawia, M. S., & Engelsen, S. B. (2010). A combined nuclear magnetic resonance and molecular dynamics study of the two structural motifs for mixed-linkage β-glucans: Methyl β-cellobioside and methyl β-laminarabioside. *Carbohydrate Research*, *345*, 474–486.
Dönges, R. (1990). Nonionic cellulose ethers. *British Polymer Journal*, *23*, 315–326.
Earl, W. L., & VanderHart, D. L. (1981). Observations by high-resolution carbon-13 nuclear magnetic resonance of cellulose I related to morphology and crystal structure. *Macromolecules*, *14*, 570–574.
Edgar, K. J., Buchanan, C. M., Debenham, J. S., Rundquist, P. A., Seiler, B. D., Shelton, M. C., et al. (2001). Advances in cellulose ester performance and application. *Progress in Polymer Science*, *16*, 1605–1688.
Flugge, L. A., Blank, J. T., & Petillo, P. A. (1999). Isolation, modification, and NMR assignments of a series of cellulose oligomers. *Journal of the American Chemical Society*, *121*, 7228–7238.
Gidley, M. J., & Bociek, S. M. (1988). ^{13}C CP/MAS studies of amylase inclusion complexes, cyclodextrins, and the amorphous phase of starch granules: Relationships between glucosidic linkage conformation and solid-state ^{13}C chemical shifts. *Journal of the American Chemical Society*, *110*, 3820–3829.
Goddard, T. D., & Kneller, D. G. (2007). *Sparky 3*. San Francisco: University of California. http://www.cgl.ucsf.edu/home/sparky, 21.06.2011
Gomez, J. A. C., Erler, U. W., & Klemm, D. O. (1996). 4-Methoxy substituted trityl groups in 6-O protection of cellulose: Homegeneous synthesis, characterization, detritylation. *Macromolecular Chemistry and Physics*, *197*, 953–964.
Ha, M.-A., Viëtor, R. J., Jardine, G. D., Apperley, D. C., & Jarvis, M. C. (2005). Conformation and mobility of the arabinan and galactan side-chains of pectin. *Phytochemistry*, *66*, 1817–1824.
Hediger, S., Emsley, L., & Fischer, M. (1999). Solid-state NMR characterization of hydration effects on polymer mobility in onion cell-wall material. *Carbohydrate Research*, *322*, 102–112.
Hoshino, M., Takai, M., Fukuda, K., Imura, K., & Hayashi, J. (1989). ^{13}C-NMR study of cellulose derivatives in the solid state. *Journal of Polymer Science Part A-Polymer Chemistry*, *27*, 2083–2092.
Klemm, D., Philipp, B., Heinze, T., Heinze, U., & Wagenknecht, W. (1998). (1st edition). *Comprehensive cellulose chemistry* Weinheim: Wiley-VCH.
Knaus, S., & Bauer-Heim, B. (2003). Synthesis and properties of anionic cellulose ethers: Influence of functional groups and molecular weight on flowability of concrete. *Carbohydrate Polymers*, *53*, 383–394.
Kondo, T. J. (1997). The relationship between intermolecular hydrogen bonds and certain physical properties of regioselectively substituted cellulose derivatives. *Journal of Polymer Science Part B-Polymer Physics*, *35*, 717–723.
Kono, H., Erata, T., & Takai, M. (2003). Determination of the through-bond carbon–carbon and carbon–proton connectivities of the native celluloses in the solid state. *Macromolecules*, *36*, 5131–5138.
Larsen, F. H., Byg, I., Damager, I., Diaz, J., Engelsen, S. B., & Ulvskov, P. (2011). Residue specific hydration of primary cell wall potato pectin identified by solid-state ^{13}C single-pulse MAS and CP/MAS NMR spectroscopy. *Biomacromolecules*, *12*, 1844–1850.
Metz, G., Wu, X., & Smith, S. O. (1994). Ramped-amplitude cross polarization in magic-angle-spinning NMR. *Journal of Magnetic Resonance A*, *110*, 219–227.
Raymond, S., Henrissat, B., Qui, D. T., Kvick, Å., & Chanzy, H. (1995). The crystal structure of methyl β-cellotrioside monohydrate 0.25 ethanolate and its relationship to cellulose II. *Carbohydrate Research*, *277*, 209–229.
Schaller, J., & Heinze, T. (2005). Studies on the synthesis of 2,3-O-hydroxyalkyl ethers of cellulose. *Macromolecular Bioscience*, *5*, 58–63.
Tan, I., Flanagan, B. M., Halley, P. J., Whittaker, A. K., & Gidley, M. J. (2007). A method for estimating the nature and relative proportions of amorphous, single and double-helical components in starch granules by ^{13}C CP/MAS NMR. *Biomacromolecules*, *8*, 885–891.
VanderHart, D. L., & Atalla, R. H. (1984). Studies of microstructure in native celluloses using solid-state ^{13}C NMR. *Macromolecules*, *17*, 1465–1472.
Wada, M., Heux, L., Nishiyama, Y., & Langan, P. (2009). X-ray crystallographic, scanning microprobe X-ray diffraction, and cross-polarized/magic angle spinning ^{13}C NMR studies of the structure of cellulose III_{II}. *Biomacromolecules*, *10*, 302–309.
Wirick, M. G. (1968). Study of the substitution pattern of hydroxyethylcellulose and its relationship to enzymic degradation. *Journal Of Polymer Science Part A-Polymer Chemistry*, *6*, 1705–1718.
Witter, R., Sternberg, U., Hesse, S., Kondo, T., Koch, F.-T., & Ulrich, A. S. (2006). ^{13}C chemical shift constrained crystal structure refinement of cellulose I_α and its verification by NMR anisotropy experiments. *Macromolecules*, *39*, 6125–6132.